ACS OMEGA

Open Access

http://pubs.acs.org/journal/acsodf

Article

Development of a Biodegradable Ternary Blend of Poly(vinyl alcohol) and Polyhydroxybutyrate Functionalized with Triacetin for Agricultural Mulch Applications

Anjana, Shristhi Rawat, and Saswata Goswami*

Cite This: *ACS Omega* 2024, 9, 30169−30182

Read Online

ACCESS | Metrics & More | Article Recommendations

ABSTRACT: The development of biodegradable mulch for agricultural applications represents a sustainable approach to reducing plastic pollution. Poly(vinyl alcohol) (PVA) is one of the nontoxic and biodegradable polymers that can be used as mulching film. However, a major drawback of PVA is its moisture sensitivity, which limits its applications. In this study, a biocomposite based on PVA and polyhydroxybutyrate (PHB), plasticized with triacetin, was developed by solvent casting method. The biocomposite film exhibited good mechanical properties, better integrity, reduced transmittance, and light-blocking properties, which can prevent weed growth. Additionally, an improvement in surface characteristics was observed, as demonstrated by the shift in contact angle from 44 to 99° and a reduction in the water vapor transmission rate (WVTR) from 4.82 to 2.31 g/h m^2. For agronomic application, the developed films were experimentally applied as mulch for maize plants in pots. The results were positive, showing that the mulches effectively supported the growth of the maize plants. Further, signs of initial degradation were observed after 5 days, and the film reached a degradation level of 50−55% after 30 days under natural conditions. Thus, this work has provided new insights for expanding the application range of PVA films in biobased mulching materials.

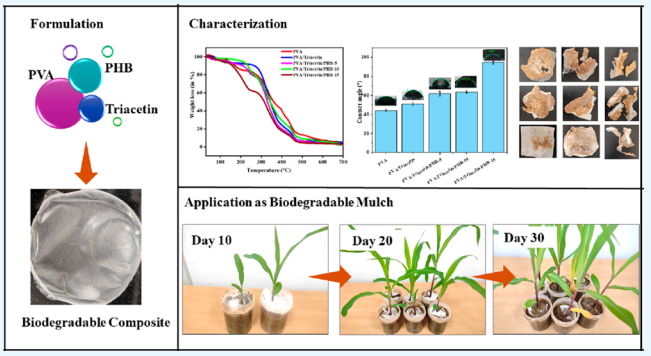

1. INTRODUCTION

In recent years, there has been a continuous increase in the global utilization of plastic mulch films. Mulches are applied to the top layer of soil in agricultural fields before, during or immediately after sowing. They are primarily used to reduce evaporation or water erosion, raise the soil temperature, increase the capacity of the soil to hold water and mitigate weed germination and vegetation restoration on severely burned forest sites.[1,2] Even though plastic mulch provides many economic and functional benefits, one major side effect is that its traces are left in the soil after harvest. The setup and removal procedures for these mulch films are costly and time-consuming. Therefore, without sufficient regulations, farmers burn most of the leftover residues on the fields, resulting in the production of mulch waste known as "white pollution". The further degradation of these plastics converts them to microplastics (particles of less than 5 mm). These residual films in the soil can affect plant growth by limiting nutrient and water uptake by roots.[3,4]

One way to reduce plastic mulch pollution in agro-ecosystems is by the substitution of petroleum-based plastic with biodegradable mulches.[5,6] Biodegradable mulches have emerged as a potential solution for the environmental friendly disposal of polyethylene crop mulch, thereby enhancing sustainability in the agricultural sector. According to the survey report, the biodegradable mulch market is anticipated to achieve a worth of $3.4 billion in 2022, with projections indicating continuous growth at a CAGR of 7.9%. By 2032, the economy is expected to reach a substantial valuation of $7.3 billion. Companies such as Bailey Bark Materials Inc., Cowart Mulch Products, Jolly Gardener, Ohio Mulch, Preen, and Woodland Mulch are involved in the production of biodegradable mulch.[7] The utilization of biobased and natural biopolymers for the development of biodegradable mulch has gained significant importance in recent times. Biobased polymers can be developed from (a) sugar-based biopolymers [e.g., polylactic acid (PLA) and poly(hydroxybutyrate) (PHB)], (b) starch-based biopolymers, (c) cellulose-based biopolymers, and (d) synthetic biopolymers [e.g., poly(ε-

Received: December 15, 2023
Revised: February 28, 2024
Accepted: May 7, 2024
Published: June 28, 2024

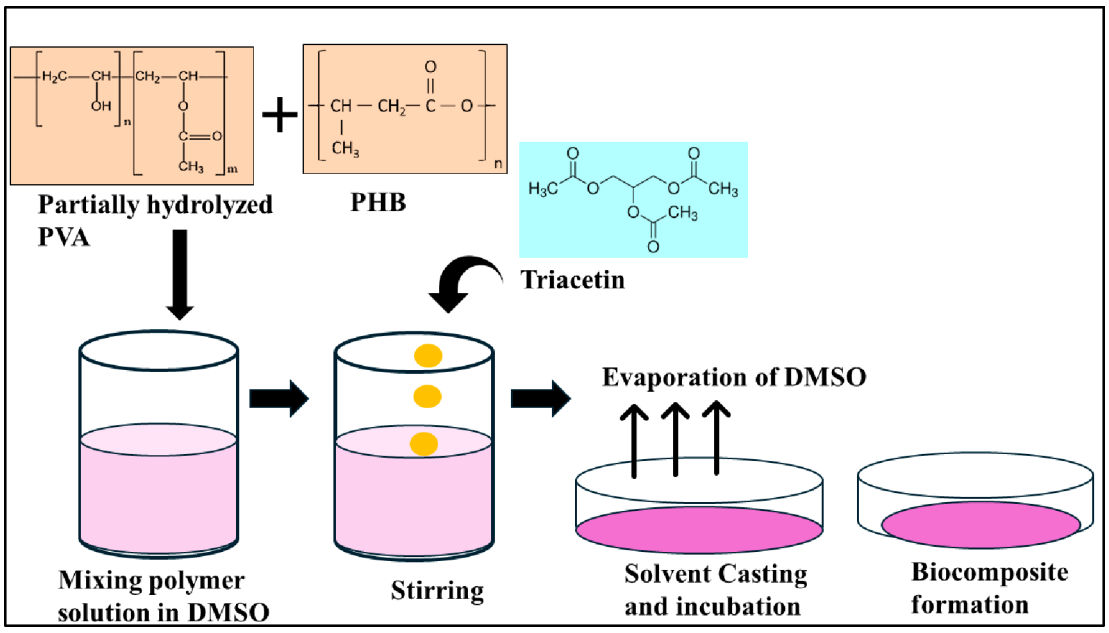

Figure 1. Schematic diagram to show the formation of a thin film of PVA reinforced with PHB and triacetin by solvent casting method.

caprolactone), poly(butylene adipate-*co*-terephthalate) (PBAT), and vinyl polymers].[8]

Among biodegradable vinyl polymers, poly(vinyl alcohol) (PVA) is a nontoxic, semicrystalline, and biodegradable polymer with abundant hydroxyl functional groups.[9] It has high flexibility, good barrier features, biocompatibility, high water solubility, and superior chemical resistance.[10] However, some constraints limit the processing of PVA for biocomposite preparation such as low processing temperature, thermal degradation, and susceptibility to humid conditions due to hydrophilicity. Various strategies have also been employed to enhance the thermal properties and hydrophobicity of PVA by lowering its melting point through blending, chemical modification, or the addition of plasticizers. The direct incorporation of hydrophobic components into a PVA solution appears to be an effective method for enhancing the hydrophobicity of PVA composites while maintaining structural stability. However, as certain additives may pose risks to the environment and ecology, it is essential to mitigate the potential hazards associated with them. The inclusion of harmful additives can negatively affect the agricultural soil environment, potentially compromising crop growth.

Previous work has demonstrated that *N*-isopropyl propionamide (NIPA)[11] and polydimethylsiloxane (PDMS)[12] can improve the hydrophobic properties by replacing the hydroxyl groups of PVA. Liu et al. coated a PVA film with monoglyceride and filled it with diatomaceous earth. The resulting reinforced PVA film exhibited the highest contact angle of 122.32° and the lowest water vapor permeability.[13] Likewise, Sun et al. utilized methyltrimethoxysilane for the hydrophobic modification of PVA aerogel fibers to enhance their structural stability and durability.[14]

Reinforcing PVA with PHB can be a suitable approach to enhance its properties, as PHB is known for its high tensile strength, biodegradability, and hydrophobicity. PHB is a biodegradable polymer derived from microbes, known for its high crystallinity and hydrophobicity. It is a semicrystalline molecule with both amorphous and crystalline phases, with the crystalline phase predominating the amorphous phase. This isotactic biopolymer bears structural similarities to isotactic polypropylene.[15] The high degree of crystallinity in PHB results from polymerization, which leads to the formation of highly organized stereochemical structured macromolecules.[16] It is typically used not in its pure form but as an ingredient in multiblended composites. PHB has a narrow processing window that can complement the PVA, thus improving several characteristics.[17] PHB exhibits mechanical properties similar to those of isotactic polyethylene, including a high Young's modulus (∼3.5 GPa) and tensile strength (∼43 MPa).[18] Since two polymers need to have similar solubility parameters (δ) to be miscible, the δ of PVA is typically 22−26 $MPa^{(1/2)}$[19,20] while that of PHB ranges from 18.5 to 20.1 $MPa^{(1/2)}$.[21,22] Therefore, good miscibility is expected due to the similar δ values of these two polymers. To date, the use of PHB as a significant hydrophobic filler to enhance the properties of PVA has not been reported. Moreover, PHB has significant potential to contribute to "The Circular Economy". This is because carbon substrates, with varying degrees of reduction and costs, can be used as raw materials for PHB synthesis. The bacterial capacity to accumulate PHB has made them highly sought after in the fermentation industries. Several bacterial genera, including *Bacillus*, *Pseudomonas*, and *Halomonas*, are capable of synthesizing PHB.[23−27]

In this context, the prior report supports the positive effects of PHB. Arrieta et al.[17] prepared a PLA blend with PHB in a ratio of 75:25 and that was later plasticized with 15 wt % acetyl(tributyl citrate) (ATBC) to show 80 times higher elongation at break compared to that of PLA. The flexibility and oxygen barrier properties were improved, along with reduced water absorption properties. Similarly, Hou et al.[28] prepared a green composite by blending PHB with PLA and poly(ethylene oxide) (PEO). It exhibited a high elongation of ∼300%, high strength (∼49 MPa), and a modulus (∼3.4 GPa) comparable to that of commercial poly(ethylene terephthalate). Its exceptional elasticity is retained even when the composite sheet has been repeatedly twisted, folded, and crumpled. Yeo et al.[29] developed another PHB/PLA-based green, reusable, and efficient sorbent by electrospinning to

https://doi.org/10.1021/acsomega.3c10027
ACS Omega 2024, 9, 30169−30182

cope with oil spillage. There were 6-fold and 30-fold enhancements in elongation and toughness (>4 MPa), respectively, due to the strong filler and matrix interaction.

To widen the processing window of PVA, a suitable plasticizer can be added to decrease its melting temperature and brittleness and improve flexibility and processability. Plasticizers enhance the free volume or segmental molecular motion of polymers, shield inter- and intra-macromolecular interactions, and reduce internal friction in the biopolymer material. Triacetin, also known as glycerol triacetate, is produced through the complete esterification of glycerol with acetic acid. It is a colorless, odorless viscous liquid and the smallest triacyl glyceride. It has a high boiling point and a low melting point. It is one of the few hydrophobic plasticizers that can enhance the barrier properties of a polymer by filling voids and creating a tortuous path in the structure.[30] Triacetin has been reported to reduce the melting point (T_m) and glass-transition temperature (T_g) of PVA, thereby improving its processability.[31]

The objective of this work is to evaluate the functionality of biobased mulching films developed from PVA and PHB. The structure−property relationships of the developed biocomposite films were studied for improved tensile strength, hydrophobicity, and low light transmittance. The tensile strength and hydrophobicity play critical roles in maintaining the integrity of mulches. Meanwhile, the low light transmittance of the film can have a positive effect on preventing soil weed growth. Later, the functional performance of the developed biocomposite as mulching films was evaluated by covering plants and observing their growth.

2. EXPERIMENTAL SECTION

2.1. Materials. White crystalline powder of cold poly(vinyl alcohol) (PVA) (with 86−89% of the degree of hydrolysis) was purchased from CDH. PVA can be categorized into three groups based on their hydrolysis level: partially hydrolyzed (80−89%), moderately hydrolyzed (90−98%), and fully hydrolyzed (98−99%). Triacetin (glyceryl triacetate), polymerized a poly[(R)-3-hydroxybutyric acid] (PHB) powder of natural origin, and dimethyl sulfoxide (DMSO) was procured from Merck, Sigma-Aldrich. Triacetin exhibited an average molecular weight (Mw) of 218 g/mol and a density of 1.16 g/cm^3 with ≥99% purity. The schematic diagram to show the formation of the biocomposite is illustrated in Figure 1.

2.2. Preparation of the Polymeric Blends. The biocomposite film was fabricated by a simple solvent casting method comprising PVA, PHB, and triacetin formulated according to the proportions outlined in Table 1. In this formulation, PVA functioned as the matrix, PHB was the filler, and triacetin played the role of a plasticizer. The polymeric blend was prepared through the solvent casting method, using DMSO as a solvent. Initially, the required amount of PHB (5−15 wt %) relative to the PVA matrix was first dissolved in DMSO by continuously stirring at 150 °C on a magnetic hot plate stirrer to obtain transparent solutions. After complete dissolution, the temperature was lowered to 100 °C, PVA was added, and the reaction continued for 1 h. Then, 3% triacetin solution was added to the PVA/PHB reaction mixture, and the reaction continued for 3−5 h. Eventually, the composite films were obtained through casting by pouring the solution onto a glass plate. The homogeneous films were obtained after drying at 55 °C in a hot air oven for 48 h. Three different synthesis batches were prepared similarly by varying the composition of PHB in the range of 5 to 15 wt %.

Table 1. Biocomposite Formulation for Prepared PVA:PHB:Triacetin Ternary Blends

Polymer blend	PVA (wt/wt %)	PHB% based on PVA concentration (wt/wt %)
PVA	100	-
PVA/triacetin	100	-
PVA/triacetin/PHB-5	95	5
PVA/triacetin/PHB-10	90	10
PVA/triacetin/PHB-15	85	15

2.3. Rheological Studies. Rheological investigations, focusing on the dynamic viscosities of the polymeric blend before solvent casting, were conducted using an Anton Paar MCR302 rheometer (Anton Paar GmbH, Graz, Austria) with a parallel plate configuration. A plate diameter of 50 mm was utilized with a measurement gap distance set at 1 mm. For each solution, 0.3 mL was poured onto the rheometer plate. Measurements were conducted at room temperature, with a shear rate ranging from 0 to 100/s at an interval of 2 s.

2.4. Light Barrier Properties. The light barrier properties of the biocomposite films were assessed by using a UV−vis spectrophotometer (UV-2600, Shimadzu, Kyoto, Japan). The transmittance %, absorption, and transmission coefficients were determined to evaluate the light barrier properties of the film in the wavelength range of 290−700 nm. The air was used as the reference/blank. The absorption and transmission coefficients are calculated according to the standard equations as described by Punde et al.[32] (eq 1) and Barani et al.[33] (eq 2), respectively.

$$\text{transmission coefficient} = \frac{|\text{sample}|^2}{|\text{blank}|^2} \quad (1)$$

$$\text{absorption coefficient} = \frac{2.303 \times \text{absorbance}}{\text{thickness of film}} \quad (2)$$

2.5. Characterization. The surface and fracture morphology of the biocomposite film were investigated using scanning electron microscopy (SEM; JEOL JCM 6000 Nikon Corporation) at an accelerated voltage of 10 kV. The functional groups were determined using Fourier transform infrared spectroscopy with attenuated total reflection (FTIR-ATR) analysis (Agilent Technologies, Carry 660 series) in the range of 450−4000 cm^{-1}. The thermal properties were determined using a thermogravimetric analyzer (TGA) and differential scanning colorimetry (DSC) (STA 8000, PerkinElmer). For TGA, samples were heated from 30 to 800 °C at a heating and cooling rate of 15 °C/min in an inert nitrogen environment. DSC measurements were conducted with a heating and cooling rate of 10 °C/min in the temperature range of 30−400 °C under a flow of nitrogen. X-ray diffraction (XRD) analysis was performed to find the crystallinity index of the biocomposite film. The samples were scanned at 2θ = 10 to 50°. The crystallinity index (CI) percentage was measured by using eq 3

$$\text{CI}(\%) = \frac{I_c}{I_c + I_A} \times 100 \quad (3)$$

where I_c is the crystalline area (2θ = 13−17, 19−20°) and I_A is the noncrystalline/amorphous region (2θ = 10−45°).

https://doi.org/10.1021/acsomega.3c10027
ACS Omega 2024, 9, 30169−30182

2.6. Mechanical Properties. The mechanical properties of test biocomposites were measured by using a universal testing machine (UTM) (Shimadzu AGX-B series) equipped with a 5 kN load cell. Preconditioned films (50 ± 5) were cut into 70 mm × 20 mm rectangles. The gauge length was 50 mm, and the test was conducted with a crosshead speed of 5 mm/min. The values of tensile strength, Young's modulus, and elongation at break (determined from the stress−strain plots) were calculated according to eqs 4, 5, and 6.[34] Tensile tests were repeated three times for each sample. All of the values were averaged, and the standard deviation was calculated.

$$\text{tensile strength} = \frac{\text{maximum tensile force}}{\text{cross-sectional area}} \quad (4)$$

$$\text{Young's modulus} = \frac{\text{stress}}{\text{strain}} \quad (5)$$

$$\text{elongation at break} = \frac{\text{total elongation of film}}{\text{initial length of film}} \times 100 \quad (6)$$

2.7. Wettability Properties. The surface wettability of the biocomposite films was investigated by utilizing static water contact angle measurements. A drop shape analyzer for contact angle measurements equipped with a camera and drop shape analysis KRÜSS ADVANCE 1.6.2.0 software was used to assess the water contact angle ($\theta°$). A sessile drop method was used to measure the contact angle at room temperature by randomly applying five drops of distilled water (~2 μL) to the film surfaces. After 30 s, the average values of five measurements for each drop were used to calculate the contact angle.[35]

2.8. Water Vapor Transmission Rate (WVTR). The WVTR of the biocomposites film was measured according to the ASTM E-96 standard method with slight modification.[36] For this, glass vials were filled with 5 g of calcium chloride. Biocomposites were applied and securely fastened with rubber bands on the vial openings. Subsequently, these vials were placed within a desiccator filled with a saturated KCl solution and maintained at a room temperature of 25 ± 2 °C and a relative humidity of 50 ± 5%. The change in the weight of the sample vials was calculated every 24 h. The WVTR was calculated using eq 7

$$\text{WVTR} = \frac{\Delta w}{\Delta t \times A} \quad (7)$$

where $\Delta w/\Delta t$ is the amount of water absorbed per unit time of transfer and A is the area exposed.

2.9. Biodegradability Study. A biodegradability study of biocomposite samples was conducted by utilizing the soil burial method in accordance with the ASTM D 6400-19 standard testing protocol.[37] A plastic pot was filled with agricultural soil with a humidity of around 50%. Then preweighed test specimen strips were buried inside for 30 days, and water was sprayed on the soil to keep it moistened. The films were removed from the soil at regular intervals. The differences in specimen weights were measured to evaluate their degradation based on weight loss %. The film weight loss was used as an indicator of degradation based on eq 8.

$$\text{weight loss \%} = \frac{\text{initial wt} - \text{final wt}}{\text{initial wt}} \times 100 \quad (8)$$

2.10. Functional Performance of the Developed Biocomposite Film as Mulch. A pot experiment was conducted to investigate the efficiency of a biocomposite as a mulch film.[38] To evaluate the mulching efficiency, maize (*Zea mays*) was selected for the experiment because of its fast germination rate. Maize seeds were planted in plastic pots (length, 150 mm; width, 100 mm; and height, 80 mm). The mulching experiment was categorized into three groups: no mulch, biocomposite mulch, and synthetic mulch. Each group had an identical total number of maize seeds, and consistent growth conditions were maintained to ensure optimal development rates. The seeds were allowed to grow under natural conditions at 30−35 °C. After the germination of seedlings, the seedlings were covered with mulch film. The growth of maize plants in the pot in all groups was monitored for 30 days, and the physiological status of the plants was finally evaluated. The plant's growth was evaluated based on the plant height measured using a measuring scale at regular intervals. The shoot and root biomass ratio was determined after sample collection and drying at 50 °C until constant weight.

3. RESULTS AND DISCUSSION

3.1. Phase Morphology and Shear Viscosity of the Ternary Blends. The mechanical behavior of a polymeric blend is greatly influenced by its phase morphology. The phase morphology depends on the concentration, properties, and interaction between the chemical constituents of the polymeric blend.[39] All of the PVA blends including different concentrations of PHB before solvent casting were subjected to phase morphological analysis. Figure 2 shows the relationship between the shear viscosity and shear rate of the polymeric blends. Each solution exhibited pseudoplastic behavior, which was strongly dependent on the concentration of PHB. The shear viscosity of each blend was the highest at the lowest shear rate, and the viscosity increased with an increase in PHB concentration. The highest apparent viscosity belongs to the PVA blend with 15% PHB, and the lowest apparent viscosity belongs to neat PVA. The dynamic viscosities of the blend

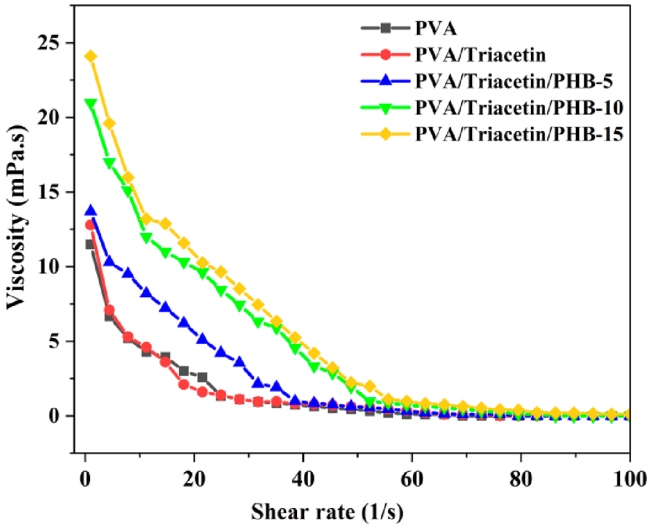

Figure 2. Viscosity vs shear rate for PVA polymeric blend components in a parallel plate rotational rheometer at room temperature.

https://doi.org/10.1021/acsomega.3c10027
ACS Omega 2024, 9, 30169−30182

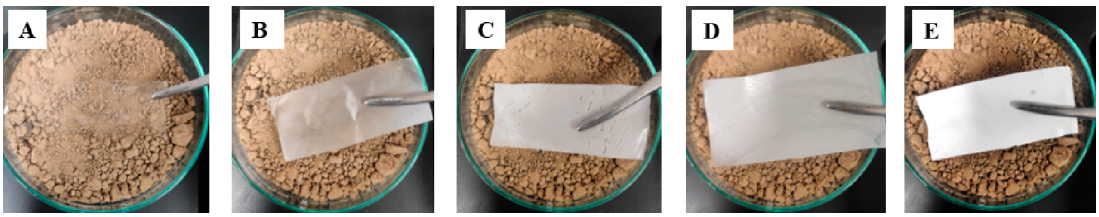

Figure 3. Physical appearance of all the PVA blends. (A) Neat PVA. (B) PVA/triacetin. (C) PVA with 5 wt % PHB. (D) PVA with 10 wt % PHB. (E) PVA with 15 wt % PHB.

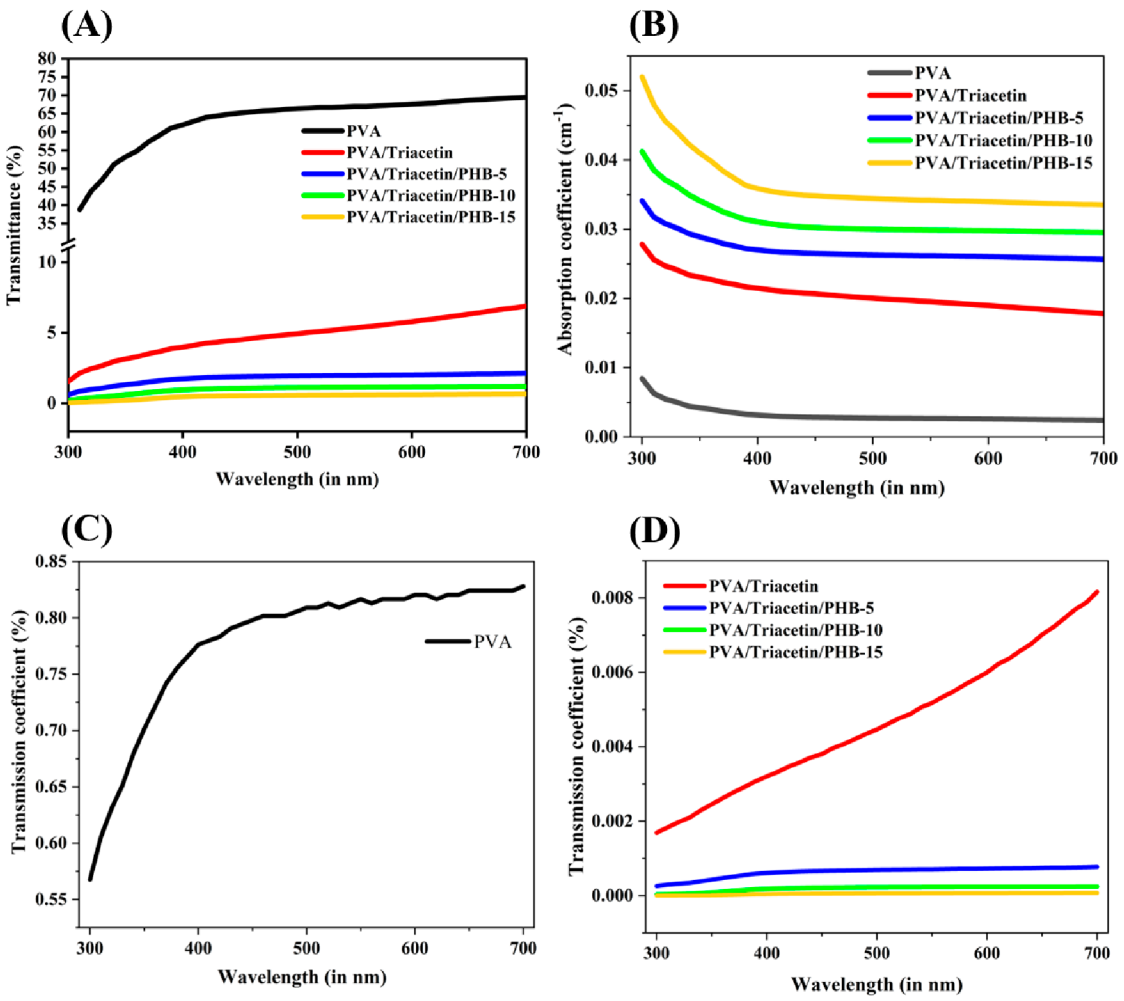

Figure 4. Spectral transmittance of PVA biocomposite films. (A) Transmittance %. (B) Light absorption coefficient. (C) Transmission coefficient of neat PVA. (D) Lower limit of the transmission coefficient (T < 0.001%) to enable the differentiation of transmission coefficients with different PHB concentrations.

containing PHB exhibited a rapid decrease at low shear rates (<50 s^{-1}), followed by a linear decrease in the range of 50−100 s^{-1}. Conversely, the viscosities of the PVA and PVA/triacetin solution without PHB exhibited a more rapid decrease below 30 s^{-1}.

These findings suggest that PHB functions as a viscous agent in the PVA solution. At high shear rates, the viscosities of all samples decrease. This behavior presents a non-Newtonian pseudoplastic fluid. Most polymers are non-Newtonian, and hence their viscosity changes with the applied shear rate. They often exhibit a phenomenon known as "shear thinning", where the viscosity decreases non-linearly as the shear rate increases. This decrease in viscosity is attributed to the alignment and disentanglement of the long polymer chains. Further, SEM was used to observe the phase separation and to characterize the phase morphology of PVA blends.

3.2. Optical Properties of the Polymeric Blend. Figure 3A−E shows the physical appearance of all PVA blends. Before solvent casting, all the blends were miscible and presented a transparent nature. When the blends were cured at 55 °C for 48 h, the neat PVA blend remained transparent, displaying a smooth and flat surface without any heterogeneity. However, after the addition of triacetin, the film's morphology exhibited significant color changes, with the surface transitioned from white to off-white. With the further addition of PHB, the biocomposite film became opaque. In multiphase blending systems, the opaque appearance implies the existence of a heterogeneous structure.[40]

https://doi.org/10.1021/acsomega.3c10027
ACS Omega 2024, 9, 30169−30182

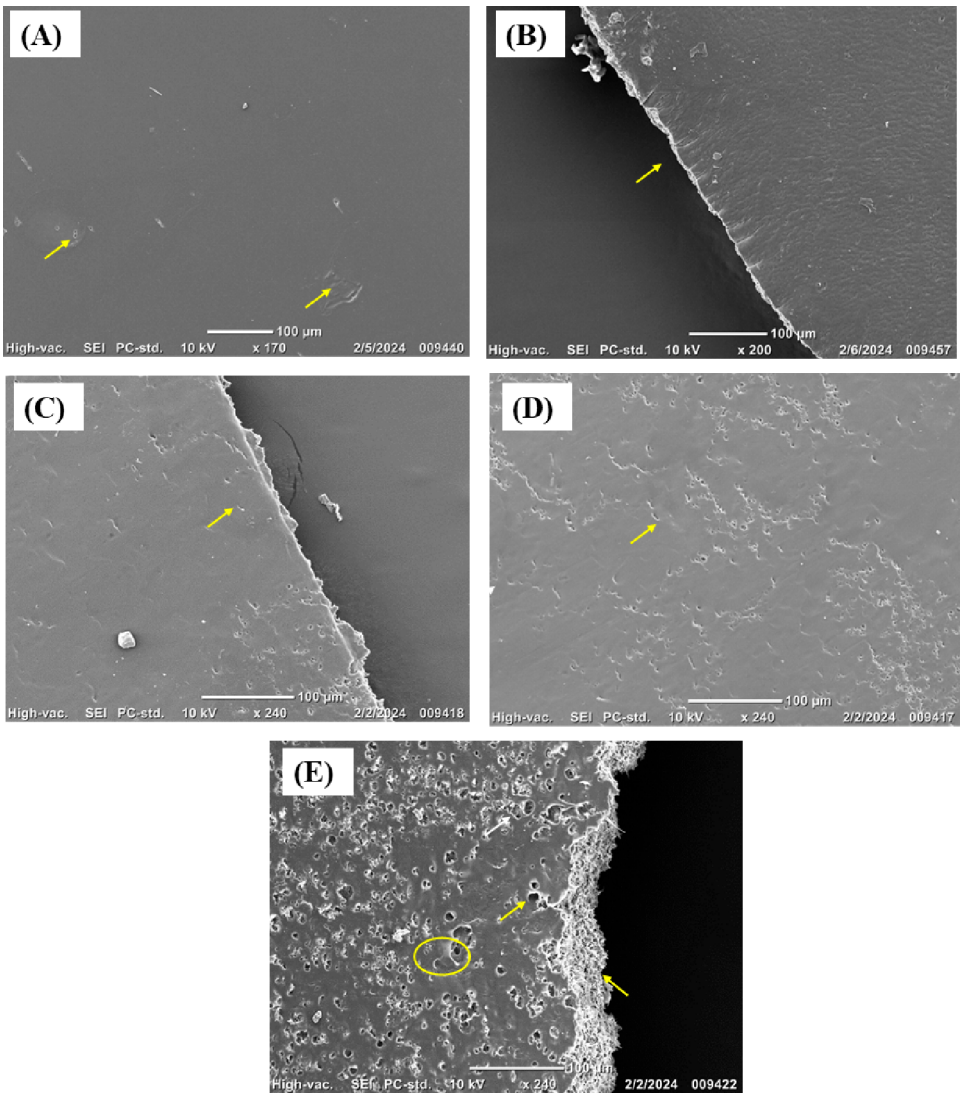

Figure 5. SEM morphology of the fractured surface of (A) neat PVA, (B) PVA/triacetin, (C) PVA with 5 wt % PHB, (D) PVA with 10 wt % PHB, and (E) PVA with 15 wt % PHB.

Figure 4A represents the UV−vis transmittance of the PVA blends measured within the range of 290−700 nm wavelength. The neat PVA film exhibited high light transparency across all wavelengths, with an excellent transparency of up to 70% at 600 nm. However, when comparing the light transmittance to that of the neat PVA biocomposite film, there was a degradation in light transmission due to the reinforcing of triacetin and PHB. The addition of triacetin reduced the light transmittance to 7%, which was further reduced to 1−5% after the addition of different concentrations of PHB. The same trend was observed for the light transmission coefficient, with neat PVA having the maximum light transmission coefficient and vice versa (Figure 4C,D). Additionally, the light absorption coefficient was maximized with the 15% PHB concentration and was at its lowest for neat PVA across all wavelengths. It decreases sequentially with a decrease in the PHB concentration (Figure 4B).

This confirms that triacetin and PHB were effective at reducing the transparency of the material. This effect can be attributed to the suppression of light scattering due to the smooth surfaces of the composites, which can be achieved by laminating an optically transparent PVA film. The three primary functions of agricultural mulches are thermal insulation, water conservation, and weed suppression. To effectively inhibit weed growth, it is necessary to have low light transmittance and a low water vapor transmission rate. The selection of the color and opacity of the plastic mulch film depends on specific targets. The typical colors of mulching films include black (the most prevalent type), transparent, and various single or dual colors used for specific cultivations. Opaque mulches reduce weed germination, conserve moisture, and prevent outgoing radiation trapped by sunlight. They prevent unwanted plant growth through resource limitation and limiting the available sunlight.[41]

3.3. Microstructure Properties. The fractured surfaces of the blends from the tensile testing samples were analyzed by using SEM to examine the phase structures. The impact-fractured surface morphology of biocomposites with various PHB concentrations is depicted in Figure 5. Pure PVA film showed a smooth and featureless fracture surface without much deformation. A similar fracture surface was observed for PVA-triacetin, but with more beach marks on the surface (marked with yellow arrows), indicating the well-distributed nature of the biocomposite throughout the entire matrix. The

https://doi.org/10.1021/acsomega.3c10027
ACS Omega 2024, 9, 30169−30182

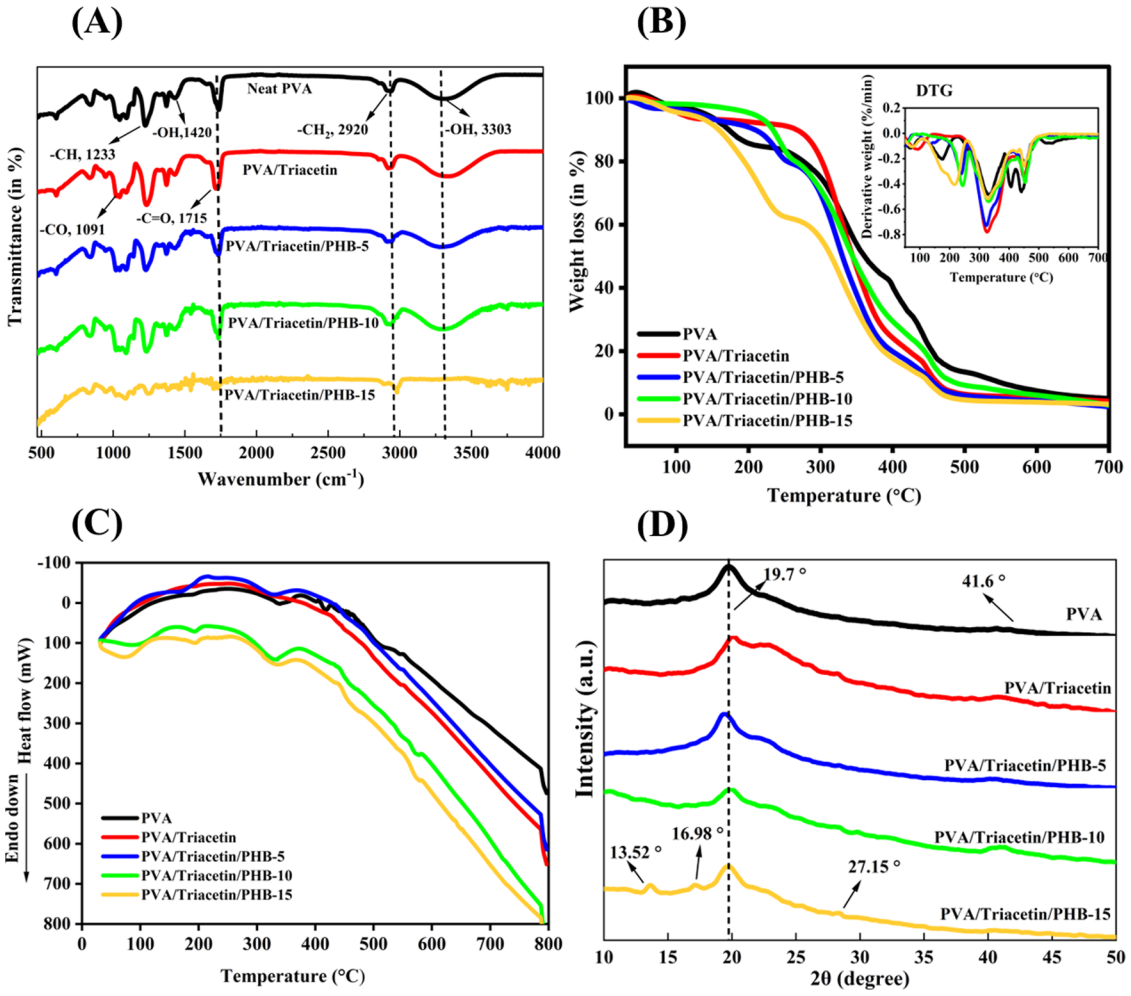

Figure 6. Characterization studies of polymeric blend with different PHB weight compositions: (A) FTIR spectra, (B) TGA-DTG curve, (C) DSC analysis, and (D) XRD spectra.

morphology of the matrix in composites with a PHB content of 5 wt % does not exhibit any phase-separated blend components between PVA and PHB. However, irregularities were evident in the blend with 10% PHB. With a PHB content of up to 15 wt %, the fractured surface structure became increasingly rugged and comprised more deformed material. These findings suggest that matrix shear yielding had taken place, deforming the PVA particles. Higher PHB content resulted in a rough morphology, with large cracks regularly and freely propagating, oriented in the direction of the load. This leads to easy crack propagation and catastrophic material failure, such as brittle materials, even under a small load. Major fracture mechanisms observed include crack pinning and deflections. Therefore, a higher PHB content, especially 15 wt %, led to compromised matrix−filler interfacial adhesion, consistent with the observed lower elongation at break. SEM analyses confirmed these findings, visually supporting the measured optical properties. A similar rupture morphology was observed for the blend of the diglycidyl ether of bisphenol A and epoxidized poly(styrene-*block*-butadiene-*block*-styrene) triblock copolymer, where crack pinning was also responsible for the fracture morphology.[42]

3.4. Functional Properties. To investigate the interaction between PVA and PHB in the films, ATR-FTIR spectroscopy was conducted. Figure 6A depicts the FTIR spectra of biocomposite film. The band at 3270−3300 cm^{-1} corresponded to the −OH stretching vibration, while the peak at 1420−1435 cm^{-1} was attributed to the −H bending vibration. The vibrational band at 2920 cm^{-1} is attributed to asymmetric stretching of the −CH$_2$ group. The band at 1715−1725 cm^{-1} is the characteristic peak of C═O stretching vibration peak due to the ester bond and carboxyl groups of PHB and triacetin, respectively. The peak attributed to −C−O stretching is located at 1091 cm^{-1}, while the band associated with the C−C stretching vibration is located at 844 cm^{-1}. The mixed bending of −CH and −OH groups corresponding to the associated alcohols was observed at 1374 cm^{-1}. The deformation vibration of the −C−O groups occurred at 1328 cm^{-1}. The peak at 1233 cm^{-1} is due to the wagging vibration of −CH groups.[43] The increase in PHB did significantly weaken the intensities of 3300, 2920, 1374, and 1092 cm^{-1} absorption bands as compared to the neat PVA. This was attributed to the formation of new hydrogen bonds among PVA, PHB, and triacetin. However, the intensity was increased at 1721 cm^{-1} due to the ester bond and carboxyl groups of PHB and triacetin. Furthermore, the bands observed with the 15 wt % PHB in the biocomposite films at 3300, 2920, 1374, and 1092 cm^{-1} associated with the −OH, −CH$_2$, −C═O, and −C−O stretching vibrations, respectively, get disrupted. This suggests that when two or more polymers are mixed, alterations in the characteristic peaks of the spectra occur due to a combination of physical blending and chemical

https://doi.org/10.1021/acsomega.3c10027
ACS Omega 2024, 9, 30169−30182

Table 2. Thermal Properties of the PVA Blend Measured with DSC

Sample	T_g	T_{m1}	ΔH_{m1} (J/g)	T_{m2}	ΔH_{m2} (J/g)
PVA	85.23	193.72	11.07	-	-
PVA/triacetin	84.21	173.06	58.73	326.05	120.41
PVA/triacetin/PHB-5	82.59	192.24	10.86	326.51	115.93
PVA/triacetin/PHB-10	84.77	197.43	88.37	326.28	101.66
PVA/triacetin/PHB-15	83.27	189.75	20.82	230.73	10.32

interactions. The primary cause appears to be the establishment of strong intermolecular hydrogen bonds and interfacial adhesion involving the −OH groups in PVA with triacetin and PHB.

3.5. Thermal Properties. Thermogravimetric analysis obtained for PVA/PHB blended films is shown in Figure 6B. Degradation has been found to occur in three stages. The TGA-DTG thermograms of neat PVA showed a single-stage degradation process.[43] The initial phase of degradation occurred at 140 °C with a 7% weight loss. This is linked to the removal of absorbed moisture and residual DMSO. The decrease in weight for PVA began at 266 °C, marked by a distinct single-step reduction at 325 °C, and peaked at 480 °C, representing 93% of the overall weight loss. After 480 °C, pyrogenic decomposition of the unstable residues generated during the initial degradation stage occured. The introduction of triacetin into the polymer blend resulted in a modification of the shape of the TGA-DTG curves. The initial degradation of the film started from 210 °C characterized by multiple steps of weight loss and reached its maximum at 480 °C. The incorporation of PHB significantly influenced the thermal stability of the PVA/triacetin blend. By increasing the PHB content from 5 to 10 wt % in the PVA/triacetin/PHB blend, the initial degradation temperature increased from 173 to 220 °C, accompanied by weight loss ranging from 6 to 9%. The second stage, marked by PHB degradation, started from 275 to 285 °C, resulting in a maximum weight loss of 80−90%. The third stage of weight loss initiated from 492 °C further pyrogenic decomposition of the unstable residues. Continuing the addition of PHB up to 15% resulted in a decrease in the degradation temperature and an increase in the weight loss percentage at each stage. The initial weight loss began at 140 °C, resulting in a 7% reduction. The second stage commenced at 250 °C with a degradation of 37%. Beyond 250 °C, the primary degradation of the PVA backbone occurred, continuing up to 473 °C and contributing to 56.3% of the total weight loss. The blends exhibited double-melting behavior, indicative of distinct melting temperatures for PVA and PHB. The presence of multiple melting peaks suggests that the polymers are not completely miscible with each other.[44] The substantial weight loss after 260 °C is attributed to the rapid breakdown of polymer segments in PVA, resulting from thermal scission of the polymer backbone. Thermal scission involves the cleavage of chemical bonds in the polymer chains due to the application of heat.

However, adding 10% PHB seems to have enhanced its thermal stability, raising the degradation temperature from 140 to 220 °C. These findings suggest that the introduction of PHB led to a reduction in the onset degradation temperature for the PHB-added blends. PHB at 10% exhibited no evidence of degradation at temperatures below 200 °C, indicating that the PVA−PHB blends demonstrated thermal stability under the specified conditions without concerns about thermal degradation.

3.6. DSC Thermograms. Figure 6C shows the DSC curves of PVA and PVA−PHB composites, emphasizing their glass-transition temperature (T_g), melting temperature (T_m), and melting enthalpy (ΔH_m), as listed in Table 2. Multiple endothermic peaks were detected in all of the samples. The first peak was assigned to T_g identified at 80−90 °C for neat PVA and PVA−PHB composites. In neat PVA, the T_g is higher than its typical value due to the absence of moisture, attributed to the use of DMSO as the solvent. The second peak corresponded to the T_m at 190−195 °C for PVA. However, the addition of triacetin reduced the T_m to 173 °C, which increased again upon further addition of PHB. For PHB-reinforced PVA composites, the T_m lies in the range of 194 °C.

The addition of PHB resulted in multiple endothermic peaks. A slight variation in the T_m was observed after PHB reinforcement, ranging from 189 to 198 °C, indicating an interaction between PHB and PVA. The slight rise in melting temperature could be attributed to the enhanced crystallinity of the composites following the addition of PHB. The increase in the T_m can be attributed to the semicrystalline nature of the material. Another sharp second endothermic melting transition temperature was observed from 326 to 338 °C. While PVA exhibited only a single T_m, PVA−PHB composites showed two T_m values. The addition of 15% PHB decreased T_{m2} to 230.73 °C. Crystallizable miscible blends often exhibit multiple DSC endotherms, attributed to phenomena such as recrystallization, secondary crystallization, or liquid−liquid phase separation. Blending two crystallizable components leads to more complex behavior due to the influence of both phases on each other. The crystallization of one phase may directly trigger crystallization in the second phase.[45]

3.7. XRD Spectra. The XRD analysis was employed to investigate the phase composition and crystallinity of the PVA composite. The XRD pattern of PVA/PHB composites are displayed in Figure 6D. The strong crystalline reflection was observed at $2\theta = 19.5°$, corresponding to the (101) crystal plane attributed to the semicrystalline nature of pure PVA. The minor peak appeared at 41.8° in the (111) crystal plane. However, the addition of triacetin to PVA leads to peak broadening with a relatively broad peak at 2θ = 22.5°. The peak broadening suggests a change in the interplanar spacing of the crystallites of the PVA matrix, likely due to the presence of triacetin. This shift indicates that the crystallites became slightly more spaced apart as the volume of triacetin increased. This change in spacing could be due to interactions between the triacetin molecules and the crystalline structure, affecting the packing of the molecules within the crystal lattice. Thus, an increase in plasticizer content enhances the interaction between the polymer and plasticizer, thereby reducing the interaction between macromolecular chains, which could impede crystallization.[46]

The diffraction profiles showed that as the PHB concentration increased from 5 to 10%, there was a systematic increase in the sharpness of the diffraction peak at $2\theta \approx 19.7°$.

https://doi.org/10.1021/acsomega.3c10027
ACS Omega 2024, 9, 30169−30182

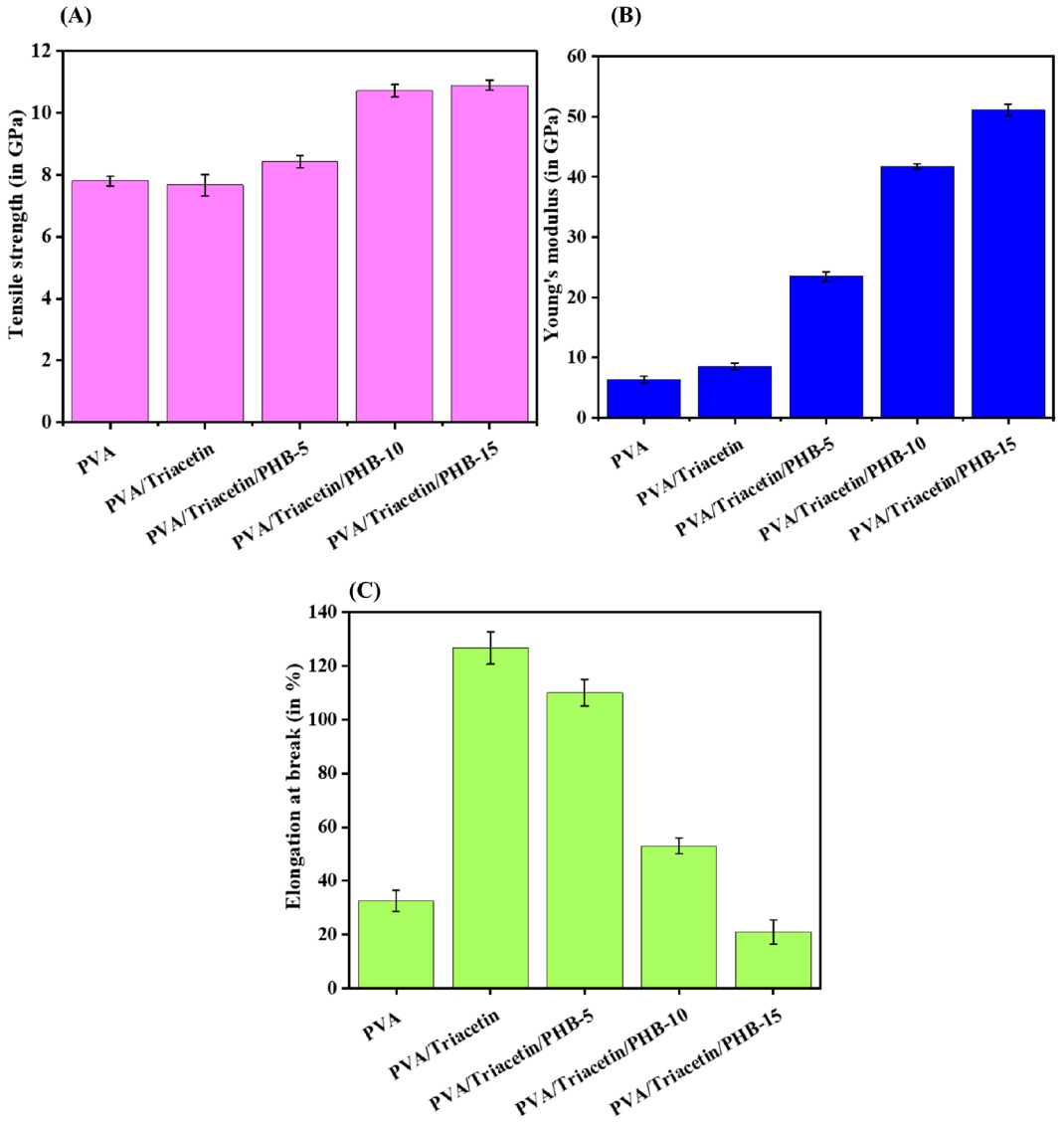

Figure 7. Determination of mechanical properties of PHB−PVA−triacetin biocomposites. (A) Ultimate tensile strength. (B) Young's modulus. (C) Elongation at break.

Following the addition of PHB, the PVA film exhibited a higher crystalline structure. The crystallinity index (CI) for neat PVA was 60.3%, which increased to 79.3% for PVA/triacetin/PHB-10 due to a more orderly and tightly packed structure. This finding is consistent with prior research and confirms the miscibility of the two polymers, likely attributed to the strong interaction between the −C═O groups of crystalline PHB and the OH groups of semicrystalline PVA, resulting in a composite film with crystalline regions. Up to 15% PHB showed a higher CI of up to 81.6%. The peaks observed at 2θ values of 13.4° (020) and 16.98° (110) corresponded to orthorhombic unit cells of PHB individually. This observation strongly indicates the highly crystalline nature of PHB. A relatively smaller peak at 27.15° (040) appeared, indicating the partially crystalline nature of PHB. The crystallinity index was comparatively higher than reported in the literature, likely due to the use of the solvent. DMSO promotes the formation of small crystals of PVA even at low temperatures, without phase separation.[47]

3.8. Mechanical Properties. The modification of PVA with triacetin and varying concentrations of PHB (5−15 wt % relative to PVA) yielded diverse mechanical properties. The impact of the PHB concentration on these properties is illustrated in Figure 7A. Neat PVA demonstrated a tensile strength of 7.8 GPa. As the PHB concentration increased from 5 to 15 wt %, the tensile strength exhibited a rapid rise, reaching 10.9 GPa. This resulted in a significant increase of 37−40% in tensile strength with the addition of 10−15% PHB. The hydroxyl groups of PVA could undergo an effective transformation into carboxyl groups, contributing to the significant enhancement of film flexibility.[48] However, without PHB, as in the PVA/triacetin blend, the tensile strength decreased from 7.8 to 7.6 GPa. In its pristine state, PVA has a Young's modulus of 6.33 GPa. The addition of triacetin increased the Young's modulus to 8.51 GPa, representing a significant 34.43% increase compared to neat PVA. The Young's modulus of the PVA matrix increased significantly, from 23.48 to 51.13 GPa, with an increase in PHB content from 5 to 15 wt %. This represented an increase of 270 to 708%, indicating the plasticizing and reinforcing effect of PHB. However, as the PHB content continued to increase, there was a gradual decline in the elongation at break (Figure 7C).

https://doi.org/10.1021/acsomega.3c10027
ACS Omega 2024, 9, 30169−30182

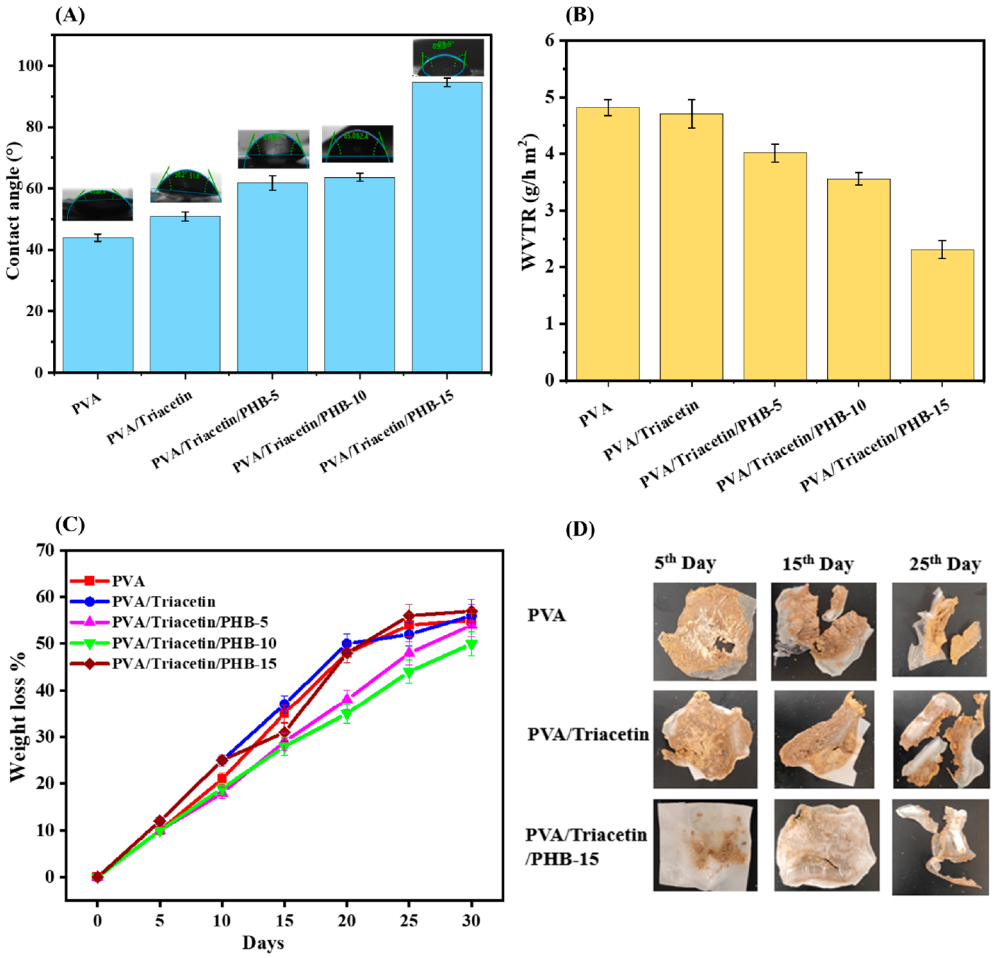

Figure 8. Surface characterization of a PVA-based biocomposite by (A) optical contact angle measurement, (B) WVTR analysis, and (C) results of soil biodegradability on different polymer blends. (D) Images of unburied film surfaces after different time intervals.

Neat PVA demonstrated a significant 32.6% elongation at break, indicating its high ductility. The addition of triacetin to PVA blends without PHB resulted in the highest elongation at the break (126.6%) among all samples. The elongation at break for PVA/triacetin was 288.3% higher than that of neat PVA. However, with the increase in PHB concentration from 5 to 10%, the elongation at break decreased from 62.5 to 237%. Beyond 10% PHB, there was a 35.5% drop in elongation at break compared to neat PVA. Consequently, the reinforcement of PHB content enhanced the tensile strength and Young's modulus of the polymer blend, although the elongation at break was inevitably weakened with PHB reinforcement exceeding 10%. The high strength of the composite indicates the high interfacial adhesion between PHB and PVA. However, the brittle nature of PHB contributed to a lower elongation at break. The process is linked to secondary crystallization, resulting in limited elongation. This phenomenon arises from its low glass-transition temperature, prompting secondary crystallization in the amorphous region at room temperature. Additionally, the low nucleation density of PHB is a significant factor contributing to the formation of interspherulitic microcracks, adversely affecting its ductile properties.[49] Higher PHB concentration led to the uneven distribution of particles and the formation of agglomerates within the polymer matrix as observed by SEM images. Thus, the polymer network was damaged, restricting the movement of the matrix and filler particles. This indicates that the PVA-based film is significantly affected by the increased PHB concentration. Among all the PVA blends, the PVA/triacetin/PHB-10 blend exhibited a balanced tensile strength and elongation at the break.

3.9. Contact Angle. Addressing the hydrophilicity of PVA is crucial for overcoming limitations in the application of PVA-based films in agriculture. To investigate water absorption on film surfaces, water contact angle measurements were conducted, as depicted in Figure 8A. Neat PVA film exhibited a smaller water contact angle value of 44°, indicating a highly hydrophilic surface. The addition of PHB, with its hydrophobic nature, led to a noticeable increase in the water contact angle, ranging from 61 to 94.6°, thereby manifesting physically facilitated hydrophobic surface behavior. The introduction of hydrophobic PHB particles into the PVA matrix seems to alter the topographical properties of the film surface. This is likely due to the hydrophobic nature of PHB, which reduces the exposure of hydrophilic −OH groups on the film surface and consequently decreases the rate of sorption of water molecules on the film structures.[50]

3.10. Water Vapor Transmission Rate (WVTR) Analysis. The WVTR test provides insights into the moisture penetration through films, and the calculated WVTR results are presented in Figure 8B. The neat PVA film exhibited the highest WVTR at 4.82 g/h m^2 among all the films. As the concentration of PHB increased from 5 to 15%, the WVTR decreased from 4.02 to 2.31 g/h m^2. The decrease in the WVTR for the PHB-reinforced film can be attributed to the

https://doi.org/10.1021/acsomega.3c10027
ACS Omega 2024, 9, 30169−30182

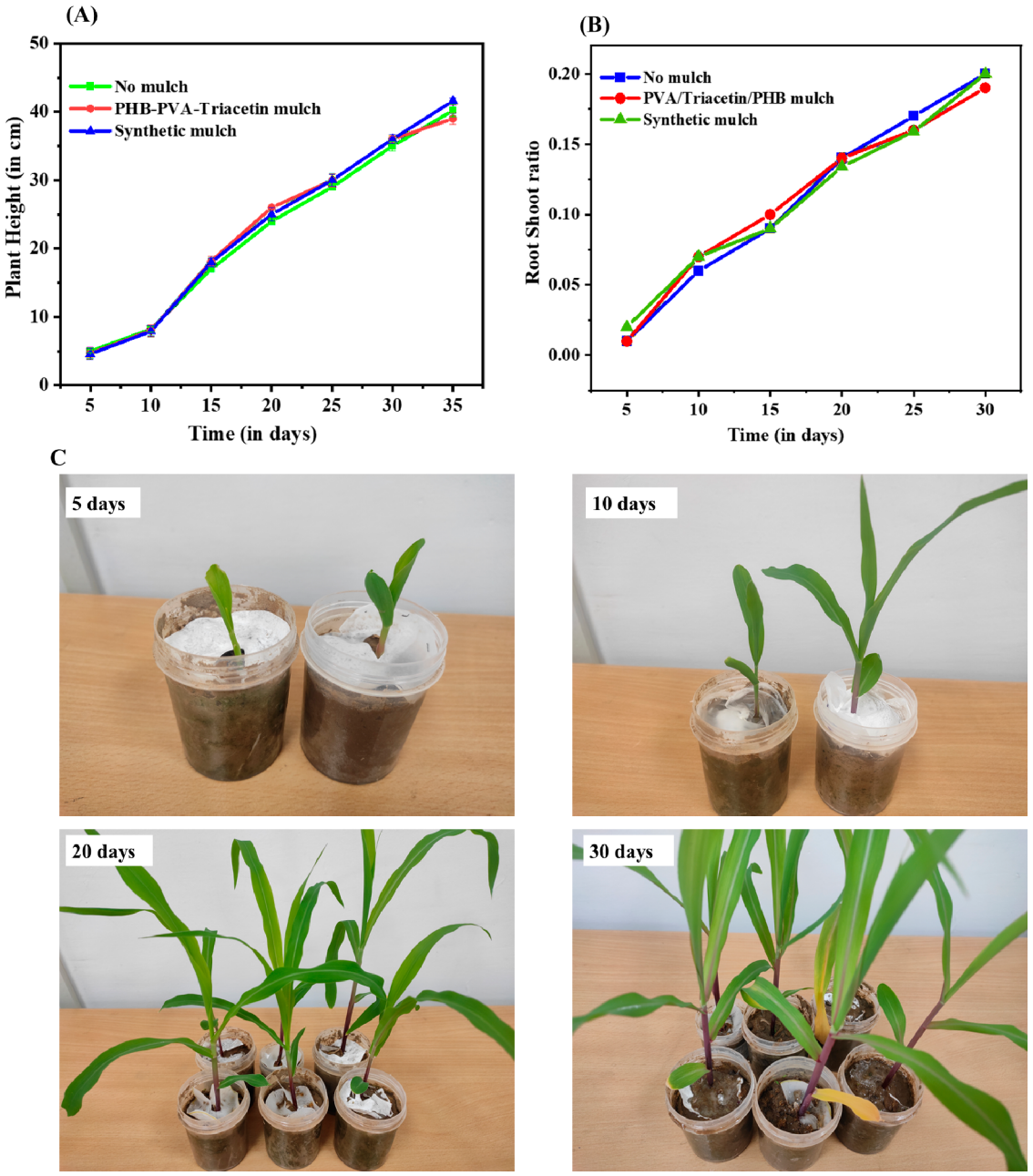

Figure 9. Effect of different mulches on the growth of plants. (A) Plant height, (B) root shoot ratio, and (C) visual appearance of plants covered with PHB-based mulch after different time intervals.

increased hydrophobicity of the polymer chains. In contrast, the WVTR increased in the neat PVA film due to its inherently hydrophilic nature. This outcome aligns with the findings of Mittal et al.[36] Therefore, the addition of PHB not only impacts the mechanical properties but also influences the water vapor transmission characteristics of the films. The gas barrier properties of mulching films play a crucial role in shaping the microenvironments of the air and soil beneath the mulch cover.

3.11. Soil Biodegradability. Soil burial degradation in soil was performed to examine the degradation of the biocomposite films under natural environmental conditions. Degradation of the specimen was reported in terms of weight loss (%) after burial in soil for 30 days. The constituent materials, PVA and PHB, used in the study are biodegradable as reported in earlier studies.[44,51] During 30 days of burial time in soil, the specimens gradually disintegrated. Figure 8C,D shows the effect of soil biodegradability on PVA/triacetin/PHB mulch film at 0, 5, 10, 15, and 20 days of degradation. It was observed that after burying the films in the soil, the size of the films decreased and the surface of the films became hard and fragile. The first sign of weight loss appeared after 5 days, followed by a slighter increase after 5 days. This suggests the easy degradation of PVA due to the high moisture sensitivity of the PVA molecule, leading to water absorption and being swollen before degradation. The degradation rate of neat PVA film was higher as compared to that of a PHB content of 5 to 10 wt % reinforced in a PVA/triacetin blend. Increasing the hydrophobicity of the films after PHB reinforcement decreased

https://doi.org/10.1021/acsomega.3c10027
ACS Omega 2024, 9, 30169−30182

the degradation rate. However, 15 wt % PHB enhanced the degradation rate.

After 25−30 days of soil burial, the polymer blend exhibited a breakdown of 50−55%, confirming its biodegradability. In this process, PHB acted as a source of carbon and energy for microbial growth, while the breakdown of PVA resulted from microbial-attack-induced random end breakage of the polymer chain. Under normal environmental conditions, water absorption typically initiates the first stage of deterioration. Subsequently, the PHB-reinforced blend is expected to undergo complete degradation, which is attributed to both microbial and oxidative deterioration processes. This emphasizes the potential of the blend as environmentally friendly and sustainable. Likewise, the inclusion of 15 wt % PHB in a PLA matrix, combined with wood particles, resulted in superior tensile, flexural, and impact characteristics compared to those of neat PLA. The introduction of PHB significantly enhanced the crystallinity of PLA, and the resulting samples exhibited biodegradability, disintegrating effectively in a compost environment.[52]

3.12. Functional Performance of Developed Biocomposite Film as Mulch on the Plant Growth. Three groups were set for the mulching experiment: group 1 was with no mulch film, group 2 covered with the PVA/triacetin/PHB mulch film, and group 3 covered with the synthetic mulch (Figure 9A−C). After the appearance of the seedlings in all the groups, they were covered with their respective mulches and allowed to grow for 30 days. The plant seedlings in each group thrived and grew luxuriantly. Moreover, the shoot/root ratio remained consistent across all cases observed for the next 30 days. This indicates that after covering the seedlings with mulch film, there were no significant changes in plant growth. Therefore, the ternary blend of PVA/triacetin/PHB demonstrated the potential for successful use as a biodegradable mulch without adversely affecting plant growth. Furthermore, these films exhibited biodegradability, showing initial signs of degradation after 5 days. Under natural conditions, they experienced further deterioration and achieved 50% degradation after 25−30 days. The degradation behavior of the PVA/triacetin/PHB-based biocomposite in soil simulating real conditions reflects the service life of the film samples intended for agricultural use. This emphasizes the environmentally friendly and sustainable nature of the mulch films.

4. DEVELOPMENT OPPORTUNITIES AND LIMITATIONS OF BIODEGRADABLE MULCHES

Even though there is growing interest in biodegradable plastics, there is still some reluctance to fully embrace them in agricultural practices. Early research and the development of biodegradable mulches often focus on polymer science, encompassing the physical and mechanical properties as well as the biodegradability of prototype films. There has been significantly less research on the agronomic performance of biodegradable mulches. The limitations in the physiochemical properties often render biodegradable polymers unsuitable for mulching in agricultural applications. The results of field-based studies can vary depending on crop species and management practices, local conditions, such as soil type and weather patterns, and mulch properties. Additionally, there are uncertainties regarding the in situ degradation of biodegradable mulches on a large scale, especially under diverse natural conditions and over extended periods, without adversely affecting plant growth. Overcoming these challenges is crucial to enhancing their effectiveness in practical use.[53]

Furthermore, enhancing the performance of the film requires the incorporation of additives. However, as certain additives may pose risks to soil ecology and crops, it is essential to mitigate the potential hazards associated with them. The inclusion of harmful additives can negatively affect the agricultural soil environment, potentially compromising crop growth. Therefore, production standards should thoroughly consider functional properties, ecological safety, crop adaptability, and other pertinent factors. The primary goal is to ensure that the final degradable film product not only meets the requirements for crop growth but also has no adverse effects on the environment. While biobased polymers and their products are usually more costly than those derived from petroleum, the lack of removal and disposal costs often balances out this expense. They have demonstrated comparable agronomic performance to that of conventional PE mulches.

5. CONCLUSIONS

The main functions of agricultural mulches include thermal insulation, water conservation, and weed suppression. To effectively hinder weed growth, it is essential to have low light transmittance and a low rate of water vapor transmission. In this study, biodegradable mulch films were prepared by blending PVA, PHB, and triacetin through solvent casting. The developed mulches were studied for improved tensile strength, barrier properties, hydrophobicity, and low light transmittance. The tensile strength and hydrophobicity are crucial for preserving the integrity of the mulches. The reduced light transmission of the film can positively impact the prevention of weed growth in the soil.

The tensile strength and Young's modulus reached 8 to 10.9 GPa and 6.33 to 51.13 GPa, respectively. The surface behavior was improved as the contact angle and WVTR shifted from 44 to 99° and from 4.82 to 2.31 g/h m^2, respectively. Rheological tests revealed that all polymeric blends exhibited non-Newtonian pseudoplastic behavior, and this pseudoplasticity increased as the PHB content increased. Finally, the degradation rates of the film were 50−55% after 30 days under natural conditions, proving the degradation properties of the film. This study confirms that the film prepared by blending PVA, PHB, and triacetin has good mechanical and barrier properties, which provides a new way to reduce pollution from agricultural films. Thus, the biobased mulching films exhibited satisfactory overall functionality. Their characteristics provide new design opportunities for environmental friendly, efficient, and sustainable agricultural practices.

AUTHOR INFORMATION

Corresponding Author

Saswata Goswami − *Division of Chemical Engineering, Center of Innovative and Applied Bioprocessing (CIAB), Mohali, Punjab 140306, India; Department of Biotechnology, Regional Center for Biotechnology (RCB), Faridabad, Haryana 121001, India;* orcid.org/0000-0001-9126-0761; Email: saswatagoswami2015@gmail.com

Authors

Anjana − *Division of Chemical Engineering, Center of Innovative and Applied Bioprocessing (CIAB), Mohali, Punjab 140306, India; Department of Biotechnology,*

https://doi.org/10.1021/acsomega.3c10027
ACS Omega 2024, 9, 30169−30182

Regional Center for Biotechnology (RCB), Faridabad, Haryana 121001, India

Shristhi Rawat − *Department of Bioscience & Bioengineering, Indian Institute of Technology (IIT), Jodhpur 342011, India*

Complete contact information is available at: https://pubs.acs.org/10.1021/acsomega.3c10027

Author Contributions

Anjana: Investigation, methodology, writing−original draft, and manuscript editing and reviewing. **Shristhi Rawat:** Methodology, instrumentation, and data curation. **Saswata Goswami:** Conceptualization, supervision, reviewing, editing of original manuscript, and resources.

Notes

The authors declare no competing financial interest.

■ ACKNOWLEDGMENTS

The authors acknowledge the Center of Innovative and Applied Bioprocessing (CIAB), Mohali for equipment and research facilities. They also acknowledge the DST-INSPIRE and DBT, Ministry of India, for funding acquisition.

■ REFERENCES

(1) Bilck, A. P.; Grossmann, M. V. E.; Yamashita, F. Biodegradable mulch films for strawberry production. *Polym. Test.* **2010**, *29* (4), 471−476.

(2) Lucas Borja, M. E.; Zema, D. A. Short-term effects of post-fire mulching with straw or wood chips on soil properties of semi-arid forests. *Journal of Forestry Research* **2023**, *34* (6), 1777−1790.

(3) Yang, Y.; Li, Z.; Yan, C.; Chadwick, D.; Jones, D. L.; Liu, E.; Liu, Q.; Bai, R.; He, W. Kinetics of microplastic generation from different types of mulch films in agricultural soil. *Science of The Total Environment* **2022**, *814*, No. 152572.

(4) Qi, Y.; Yang, X.; Pelaez, A. M.; Huerta Lwanga, E.; Beriot, N.; Gertsen, H.; Garbeva, P.; Geissen, V. Macro- and micro- plastics in soil-plant system: Effects of plastic mulch film residues on wheat (Triticum aestivum) growth. *Science of The Total Environment* **2018**, *645*, 1048−1056.

(5) Yin, M.; Li, Y.; Fang, H.; Chen, P. Biodegradable mulching film with an optimum degradation rate improves soil environment and enhances maize growth. *Agric. Water Manage.* **2019**, *216*, 127−137.

(6) Li, B.; Huang, S.; Wang, H.; Liu, M.; Xue, S.; Tang, D.; Cheng, W.; Fan, T.; Yang, X. Effects of plastic particles on germination and growth of soybean (Glycine max): A pot experiment under field condition. *Environ. Pollut.* **2021**, *272*, No. 116418.

(7) https://www.factmr.com/report/1005/mulching-materials-market, 2022.

(8) Bhagabati, P. In *Sustainable Nanocellulose and Nanohydrogels from Natural Sources*; Mohammad, F., Al-Lohedan, H. A., Jawaid, M., Eds.; Elsevier: 2020; Chapter 9, pp 197−216.

(9) Abdullah, Z. W.; Dong, Y.; Davies, I. J.; Barbhuiya, S. PVA, PVA blends, and their nanocomposites for biodegradable packaging application. *PPTEn* **2017**, *56* (12), 1307−1344.

(10) Terzioğlu, P.; Parın, F. N. Polyvinyl Alcohol-Corn Starch-Lemon Peel Biocomposite Films as Potential Food Packaging. *Celal Bayar Üniversitesi Fen Bilimleri Dergisi* **2020**, *16*, 373−378.

(11) Liu, F.; Cao, Y.; Zhang, Y.; Xie, Y.; Xu, H.; Dong, X.; Liu, Y.; Wang, Q.; Jiao, W.; Alee, M.; Xiao, X. Preparation and characterization of N-isopropyl acrylamide grafted polyvinyl alcohol and chitosan blend films with hydrophobic and antibacterial properties. *React. Funct. Polym.* **2023**, *188*, No. 105604.

(12) Yang, R.; Li, X. Functionalized PVA/PDMS-Modified Nanocomposite Electrospun Film with Tertiary Roughness for Humid and Bacterial Applications. *Fibers Polym.* **2023**, *24* (4), 1237−1251.

(13) Liu, F.; Li, C.; Liu, C.; Zheng, J.; Bian, K.; Bai, H.; Zhang, Y.; Cao, Y.; Xie, Y.; Xiao, X. Improvement of Hydrophobicity and Gas Permeability of the Polyvinyl Alcohol Film Utilizing Monoglyceride Coating and Diatomaceous Earth Filling and Its Application to Fresh-Cut Mango. *ACS Sustainable Chem. Eng.* **2023**, *11* (29), 10938−10949.

(14) Sun, T.; Zhang, W.; Liu, Y.; Xu, W.; Sun, J.; Wang, J.; Qin, C.; Dai, L. Preparation of high-hydrophobic polyvinyl alcohol-based composite aerogel fibers containing organosilicon for effective thermal insulation. *Polym. Adv. Technol.* **2024**, *35* (1), No. e6198.

(15) Volova, T. G.; Uspenskaya, M. V.; Kiselev, E. G.; Sukovatyi, A. G.; Zhila, N. O.; Vasiliev, A. D.; Shishatskaya, E. I. Effect of Monomers of 3-Hydroxyhexanoate on Properties of Copolymers Poly(3-Hydroxybutyrate-co 3-Hydroxyhexanoate). *Polymers [Online]* **2023**, *15*, 2890.

(16) Menossi, M.; Cisneros, M.; Alvarez, V. A.; Casalongué, C. Current and emerging biodegradable mulch films based on polysaccharide bio-composites. A review. *Agronomy for Sustainable Development* **2021**, *41* (4), 53.

(17) Arrieta, M. P.; López, J.; López, D.; Kenny, J. M.; Peponi, L. Biodegradable electrospun bionanocomposite fibers based on plasticized PLA−PHB blends reinforced with cellulose nanocrystals. *Industrial Crops and Products* **2016**, *93*, 290−301.

(18) Zhuikova, Y.; Zhuikov, V.; Varlamov, V. Biocomposite Materials Based on Poly(3-hydroxybutyrate) and Chitosan: A Review. *Polymers (Basel)* **2022**, *14* (24), 5549.

(19) Chen, S.; Yang, H.; Huang, K.; Ge, X.; Yao, H.; Tang, J.; Ren, J.; Ren, S.; Ma, Y. Quantitative Study on Solubility Parameters and Related Thermodynamic Parameters of PVA with Different Alcoholysis Degrees. *Polymers [Online]* **2021**, *13*, 3778.

(20) Rudin, A.; Choi, P. Polymer Mixtures. *Elements of Polymer Science & Engineering* **2013**, 231−274.

(21) Patel, M. K.; Hansson, F.; Pitkänen, O.; Geng, S.; Oksman, K. Biopolymer Blends of Poly(lactic acid) and Poly(hydroxybutyrate) and Their Functionalization with Glycerol Triacetate and Chitin Nanocrystals for Food Packaging Applications. *ACS Appl. Polym. Mater.* **2022**, *4* (9), 6592−6601.

(22) Arrieta, M. P.; Perdiguero, M.; Fiori, S.; Kenny, J. M.; Peponi, L. Biodegradable electrospun PLA-PHB fibers plasticized with oligomeric lactic acid. *Polym. Degrad. Stab.* **2020**, *179*, No. 109226.

(23) Anjana; Raturi, G.; Shree, S.; Sharma, A.; Panesar, P. S.; Goswami, S. Recent approaches for enhanced production of microbial polyhydroxybutyrate: Preparation of biocomposites and applications. *Int. J. Biol. Macromol.* **2021**, *182*, 1650−1669.

(24) Anjana; Rawat, S.; Goswami, S. In-silico analysis of a halophilic bacterial isolate-Bacillus pseudomycoides SAS-B1 and its polyhydroxybutyrate production through fed-batch approach under differential salt conditions. *Int. J. Biol. Macromol.* **2023**, *229*, 372−387.

(25) Anjana; Rawat, S.; Goswami, S. Synergistic approach for enhanced production of polyhydroxybutyrate by Bacillus pseudomycoides SAS-B1: Effective utilization of glycerol and acrylic acid through fed-batch fermentation and its environmental impact assessment. *Int. J. Biol. Macromol.* **2024**, *258*, No. 128764.

(26) Chandra, R.; Thakor, A.; Mekonnen, T. H.; Charles, T. C.; Lee, H.-S. Production of polyhydroxyalkanoate (PHA) copolymer from food waste using mixed culture for carboxylate production and Pseudomonas putida for PHA synthesis. *Journal of Environmental Management* **2023**, *336*, No. 117650.

(27) Hathi, Z. J.; Haque, M. A.; Priya, A.; Qin, Z.-h.; Huang, S.; Lam, C. H.; Ladakis, D.; Pateraki, C.; Mettu, S.; Koutinas, A.; Du, C.; Lin, C. S. K. Fermentative bioconversion of food waste into biopolymer poly(3-hydroxybutyrate-co-3-hydroxyvalerate) using Cupriavidus necator. *Environmental Research* **2022**, *215*, No. 114323.

(28) Hou, X.; Liu, S.; He, C. Designing ultratough, malleable and foldable biocomposites for robust green electronic devices. *Journal of Materials Chemistry A* **2022**, *10* (3), 1497−1505.

(29) Yeo, J. C. C.; Kai, D.; Teng, C. P.; Lin, E. M. J. R.; Tan, B. H.; Li, Z.; He, C. Highly Washable and Reusable Green Nanofibrous Sorbent with Superoleophilicity, Biodegradability, and Mechanical Robustness. *ACS Applied Polymer Materials* **2020**, *2* (11), 4825−4835.

(30) Eslami, Z.; Elkoun, S.; Robert, M.; Adjallé, K. A Review of the Effect of Plasticizers on the Physical and Mechanical Properties of Alginate-Based Films. *Molecules [Online]* **2023**, *28*, 6637.
(31) Zuber, S. A. N. A.; Rusli, A.; Ismail, H. Effectiveness of triacetin and triethyl citrate as plasticizer in polyvinyl alcohol. *Materials Today: Proceedings* **2019**, *17*, 560−567.
(32) Punde, A. L.; Shah, S. P.; Hase, Y. V.; Waghmare, A. D.; Shinde, P. S.; Bade, B. R.; Pathan, H. M.; Prasad, M.; Patole, S. P.; Jadkar, S. Self-biased photodetector using 2D layered bismuth triiodide (BiI(3)) prepared using the spin coating method. *RSC Adv.* **2022**, *12* (46), 30157−30166.
(33) Barani, Z.; Kargar, F.; Godziszewski, K.; Rehman, A.; Yashchyshyn, Y.; Rumyantsev, S.; Cywiński, G.; Knap, W.; Balandin, A. A. Graphene Epoxy-Based Composites as Efficient Electromagnetic Absorbers in the Extremely High-Frequency Band. *ACS Appl. Mater. Interfaces* **2020**, *12* (25), 28635−28644.
(34) Wu, Z.; Huang, Y.; Xiao, L.; Lin, D.; Yang, Y.; Wang, H.; Yang, Y.; Wu, D.; Chen, H.; Zhang, Q.; Qin, W.; Pu, S. Physical properties and structural characterization of starch/polyvinyl alcohol/graphene oxide composite films. *Int. J. Biol. Macromol.* **2019**, *123*, 569−575.
(35) Agüero, Á.; Corral Perianes, E.; Abarca de las Muelas, S. S.; Lascano, D.; de la Fuente García-Soto, M. D.; Peltzer, M. A.; Balart, R.; Arrieta, M. P. Plasticized Mechanical Recycled PLA Films Reinforced with Microbial Cellulose Particles Obtained from Kombucha Fermented in Yerba Mate Waste. *Polymers [Online]* **2023**, *15*, 285.
(36) Mittal, A.; Garg, S.; Kohli, D.; Maiti, M.; Jana, A. K.; Bajpai, S. Effect of cross linking of PVA/starch and reinforcement of modified barley husk on the properties of composite films. *Carbohydr. Polym.* **2016**, *151*, 926−938.
(37) ASTM, 6400-19 Standard Test Method for Determining Aerobic Biodegradation of Plastic Materials under Controlled Composting Condition; American Society for Testing and Materials International, 2019.
(38) Wang, K.; Sun, X.; Long, B.; Li, F.; Yang, C.; Chen, J.; Ma, C.; Xie, D.; Wei, Y. Green Production of Biodegradable Mulch Films for Effective Weed Control. *ACS Omega* **2021**, *6* (47), 32327−32333.
(39) Soltani, I.; Zeynali, M. E.; Yousefi, A. A. Toughening of glass fiber reinforced Nylon 66 with EPDMMAH: Dynamic mechanical, rheological, and morphological investigations. *e-Polym.* **2012**, *12* (1).
(40) Zhao, P.; Zhou, Q.; Liu, X.; Zhu, R.; Ran, Q.; Gu, Y. Phase separation in benzoxazine/epoxy resin blending systems. *Polym. J.* **2013**, *45* (6), 637−644.
(41) Sirivechphongkul, K.; Chiarasumran, N.; Saisriyoot, M.; Thanapimmetha, A.; Srinophakun, P.; Iamsaard, K.; Lin, Y.-T. Agri-Biodegradable Mulch Films Derived from Lignin in Empty Fruit Bunches. *Catalysts [Online]* **2022**, *12*, 1150.
(42) Remya, V. P.; Parani, S.; Sakho, E. H.; Rajendran, J. V.; Maluleke, R.; Lebepe, T. C.; Masha, S.; Hameed, N.; Thomas, S.; Oluwafemi, O. S. Highly Toughened Nanostructured Self-Assembled Epoxy-Based Material—Correlation Study between Nanostructured Morphology and Fracture Toughness—Impact Characteristics. *Polymers [Online]* **2023**, *15*, 1689.
(43) Choo, K.; Ching, Y. C.; Chuah, C. H.; Julai, S.; Liou, N. S. Preparation and Characterization of Polyvinyl Alcohol-Chitosan Composite Films Reinforced with Cellulose Nanofiber. *Materials (Basel)* **2016**, *9* (8), 644.
(44) Patel, M. K.; Hansson, F.; Pitkänen, O.; Geng, S.; Oksman, K. Biopolymer Blends of Poly(lactic acid) and Poly(hydroxybutyrate) and Their Functionalization with Glycerol Triacetate and Chitin Nanocrystals for Food Packaging Applications. *ACS Applied Polymer Materials* **2022**, *4* (9), 6592−6601.
(45) Groeninckx, G.; Harrats, C.; Vanneste, M.; Everaert, V. Crystallization, Micro- and Nano-structure, and Melting Behavior of Polymer Blends. In *Polymer Blends Handbook*; Utracki, L. A., Wilkie, C. A., Eds.; Springer: Dordrecht, 2014; pp 291−446.
(46) Zhu, J.; Li, X.; Huang, C.; Chen, L.; Li, L. Plasticization effect of triacetin on structure and properties of starch ester film. *Carbohydr. Polym.* **2013**, *94* (2), 874−881.
(47) Sakaguchi, T.; Nagano, S.; Hara, M.; Hyon, S.-H.; Patel, M.; Matsumura, K. Facile preparation of transparent poly(vinyl alcohol) hydrogels with uniform microcrystalline structure by hot-pressing without using organic solvents. *Polym. J.* **2017**, *49* (7), 535−542.
(48) Ma, Z.; Ma, Y.; Qin, L.; Liu, J.; Su, H. Preparation and characteristics of biodegradable mulching films based on fermentation industry wastes. *Int. Biodeterior. Biodegrad.* **2016**, *111*, 54−61.
(49) Garcia-Garcia, D.; Quiles-Carrillo, L.; Balart, R.; Torres-Giner, S.; Arrieta, M. P. Innovative solutions and challenges to increase the use of Poly(3-hydroxybutyrate) in food packaging and disposables. *Eur. Polym. J.* **2022**, *178*, No. 111505.
(50) Cyras, V. P.; Soledad, C. M.; Analía, V. Biocomposites based on renewable resource: Acetylated and non acetylated cellulose cardboard coated with polyhydroxybutyrate. *Polymer* **2009**, *50* (26), 6274−6280.
(51) Sukudom, N.; Jariyasakoolroj, P.; Jarupan, L.; Tansin, K. Mechanical, thermal, and biodegradation behaviors of poly(vinyl alcohol) biocomposite with reinforcement of oil palm frond fiber. *J. Mater. Cycles Waste Manage.* **2019**, *21* (1), 125−133.
(52) Pérez-Fonseca, A. A.; Herrera-Carmona, V. S.; Gonzalez-García, Y.; Martín del Campo, A. S.; González-López, M. E.; Ramírez-Arreola, D. E.; Robledo-Ortíz, J. R. Influence of the blending method over the thermal and mechanical properties of biodegradable polylactic acid/polyhydroxybutyrate blends and their wood biocomposites. *Polym. Adv. Technol.* **2021**, *32* (9), 3483−3494.
(53) Kasirajan, S.; Ngouajio, M. Polyethylene and biodegradable mulches for agricultural applications: a review. *Agronomy for Sustainable Development* **2012**, *32* (2), 501−529.

https://doi.org/10.1021/acsomega.3c10027
ACS Omega 2024, 9, 30169−30182